


Cetuximab–siRNA Conjugate Linked Through Cationized Gelatin Knocks Down KRAS G12C Mutation in NSCLC Sensitizing the Cells Toward Gefitinib

Technology in Cancer Research & Treatment
Volume 20: 1-17
© The Author(s) 2021
Article reuse guidelines:
sagepub.com/journals-permissions
DOI: 10.1177/15330338211041453
journals.sagepub.com/home/tct


K. Sreedurgalakshmi, M.Tech^{1,2}, R. Srikar, PhD² , K. Harikrishnan, MSc², Lakshmi Srinivasan, B.Tech², and Reena Rajkumari, PhD¹

Abstract

Delivery of small-interfering RNA (siRNA) has been of great interest in the past decade for effective gene silencing. To overcome synthetic and regulatory challenges posed by nanoparticle-mediated siRNA delivery, antibody–siRNA conjugate (ARC) platform is emerging as a potential siRNA delivery system suitable for clinical translation. Herein, we have developed a delivery technology based on the ARC platform for stable delivery of siRNA called as Gelatin-Antibody Delivery System (GADS). In GADS, positively charged gelatin acts as a linker between antibody–siRNA and enables the endosomal escape of siRNA for gene silencing postcellular internalization. For proof of concept, we synthesized a scalable GADS conjugate comprising of Cetuximab (CTB), cationized gelatin (cGel) and NSCLC KRAS_{G12C}-specific siRNA. CTB was chemically conjugated to cGel through an amide link to form the CTB–cGel complex. Thereafter, siRNA was chemically conjugated to the cGel moiety of the complex through the thioether link to form CTB–cGel–siRNA conjugate. RP-HPLC analysis was used to monitor the reaction while gel retardation assay was used to determine siRNA loading capacity. SPR analysis showed the preservation of ligand binding affinity of antibody conjugates with K_D of ~0.3 nM. Furthermore, cellular internalization study using fluorescent microscopy revealed receptor-mediated endocytosis. The conjugate targeted EGFR receptor of KRAS mutant NSCLC to specifically knockdown G12C mutation. The oncogene knockdown sensitized the cells toward small molecule inhibitor—Gefitinib causing ~70% loss in cell viability. Western blot analysis revealed significant downregulation for various RAS downstream proteins postoncogene knockdown. Comparison of the efficiency of GADS vis-à-vis positive siRNA control and CRISPR–Cas9-based knockout of KRAS Exon 2 in the NCI-H23 NSCLC cell line suggests GADS as a potential technology for clinical translation of gene therapy.

Keywords

cancer therapy, lung cancer, gene, RNAi, drug delivery

Abbreviations

siRNA, small-interfering RNA; NSCLC, non-small cell lung cancer; CTB, cetuximab; cGEL, cationized gelatin; si(TA), transfected siRNA using lipofectamine; GADS, gelatin-antibody delivery system; SPR, surface plasmon resonance; RP-HPLC, reverse-phase high-pressure liquid chromatography; TKI, tyrosine kinase inhibitor; CRISPR, clustered regularly interspaced small palindromic repeats; RISC, RNA-induced silencing complex; API, active pharmaceutical ingredient; mAb, monoclonal antibody

Received: March 18, 2021; Revised: August 2, 2021; Accepted: August 4, 2021.

Introduction

Small-interfering RNA (siRNA) is a promising therapeutic tool for genetic diseases such as cancer, wherein several types of carcinomas are either undruggable or develop secondary mutations leading to drug resistance.^{1–3} Knocking down the oncogene of interest circumvents the druggability issues enabling effective personalized therapies.⁴ siRNA is known for effective

¹ Vellore Institute of Technology, Vellore, Tamil Nadu, India
² R&D, Levim Biotech LLP, Chennai, Tamil Nadu, India

Corresponding Authors:

R. Srikar, Division of Biosimilars and Gene Therapy, R&D, Levim Biotech LLP, Chennai, Tamil Nadu, India.
Email: srikar@levimbiotech.com

Reena Rajkumari, School of Biosciences and Technology, Vellore Institute of Technology, Vellore, Tamilnadu, India.
Email: b.reenarajkumari@vit.ac.in



knockdown of cytoplasmic genes with high specificity that leads to either cellular apoptosis or drug sensitization. However, their clinical application is restricted due to its low *in vivo* stability.^{5,6} Also, cytoplasmic localization of siRNA is required for siRNA to bind with RNA-induced silencing complex (RISC) for effecting mRNA knockdown.⁶ Cytoplasmic translocation requires endosomal escape after cellular internalization which is generally achieved if the molecule of interest is either cationic or has charge reversal properties.^{7,8} Indeed, in the past decade, the need for stability and cytoplasmic translocation has generated interest on the stable delivery of siRNA for utilizing its therapeutic potential. Several works have been reported on modalities to protect siRNA from external degradation factors and effect stable delivery within the cytoplasm of cells for effective gene silencing.^{4,9}

Systems reported for delivery of siRNA can be broadly classified into the viral delivery system or non-viral delivery system. In the case of non-viral systems, nanoparticle (NP) platform comprising of metallic, polymeric, or liposomal-based systems have been explored.^{8,10–12} For metallic systems, gold nanoparticle (AuNP) mediated siRNA delivery has been of primary focus.^{13,14} However, the relevance of AuNP delivery system for clinical translation, specifically for the delivery of siRNA, is limited due to siRNA degradation and bioavailability. Nonetheless, few works have been reported to address the issues to certain extent through surface layering.^{7,14,15} In the case of polymeric NP delivery systems, advancements in drug encapsulation techniques and controlled release of drugs provide synthetic design advantages over metallic NPs.^{16,17} For delivery of siRNA, the biomolecule is physically entrapped within polymeric NPs and targeted to biomarkers. Several works have been reported on the use of cationic polymers such as Polyethyleneimine (PEI) and Cyclodextrin for designing such systems.^{18–21} However, the use of PEI as the siRNA delivery system is restricted due to dose-dependent toxicity. Also, with few exceptions of polymer-based siRNA delivery platform, encapsulation of large molecules for systemic delivery is synthetically challenging.²²

To move beyond NP-mediated delivery of siRNA, other alternate methods have been explored such as direct conjugation of siRNA to ligands through linkers or embedding the macromolecule within biodegradable matrix.^{22–26} Such techniques provide relatively higher control and precision on the composition yielding homogeneous formulations. Using the embedding technique, Khvalevsky et al. reported an implantable platform—LODER, for siRNA-mediated knockdown *in vivo*.²² LODER is an intratumor implantable device comprising of biodegradable polymer matrix that protects siRNA from serum degradation and releases siRNA over an extended period, albeit without targeting.

For targeted delivery of siRNA, the use of ligands, such as antibody or peptide linked to siRNA, is a potential solution. Similar to Antibody Drug Conjugate (ADC) and called as antibody–siRNA conjugates (ARC), ligands linked to siRNA is emerging as one of the leading platforms for siRNA delivery.

Ligands such as antibody, antibody fragments, peptides, and aptamers have been commonly used for delivering siRNA.^{24,25} One such system, called Dynamic Poly-Conjugates (DPC), was reported by Rozema et al.²³ DPC was developed by conjugating siRNA to amphipathic polyvinyl ether (PBAVE) through disulfide linkage and complexed with small molecule *N*-acetylgalactosamine (GalNAc).²³ Several lead molecules have been developed for the delivery of siRNA with GalNAc that have entered clinical trials.²⁷ For targeted delivery, Cuellar et al.²⁶ reported direct linking of siRNA to antibody using THIOMAB technology. Based on the ARC platform, the system comprised antibody linked to siRNA through a small molecule sulfo-SMCC linker. However, the effective oncogene knockdown of this platform was applicable only for specific systems with high antigen expression. Also, inadequate cytoplasmic translocation may be one of the primary reasons for limited gene knockdown. In a separate work, cytoplasmic translocation issue was overcome by utilizing protamine as a linker.²⁸ The system reported in the work utilized fusion protein containing positively charged protamine and single-chain variable fragment (scFv) of antibody or Fab fragment. While it is known that the lack of Fc domain induces a high risk of agglomeration during production and purification, it is important to consider cationic property in conjunction with targeting moiety for effecting successful gene knockdown while designing ARCs.

NSCLC KRAS_{G12C} mutation is known to be undruggable till date. A few small molecule inhibitors have entered clinical trials for specifically targeting G12C mutation.²⁹ However, it is known that inhibitors such as TKIs, used for EGFR mutations, cause acquired resistances by activating alternate signaling pathways.³⁰ In this work, we aimed to develop an effective and scalable ARC through Gelatin-Antibody Delivery System (GADS) technology for circumventing drug resistance through gene knockdown. The platform comprises (i) antibody that serves as targeting moiety and carrier, (ii) a cationic macromolecule linking siRNA to antibody as well as aiding in endosomal escape, and (iii) siRNA for gene knockdown (Figure 1).

We demonstrated the effective KRAS_{G12C} knockdown in NSCLC using cetuximab (CTB), cationized Gelatin (cGel) and siRNA (CTB–cGel–siRNA) compound. The compound was synthesized by linking carboxyl groups of cationic gelatin to lysine residues of EGFR-specific antibody-CTB through amide bond. Thiol-modified siRNA (S-S-siRNA) was subsequently conjugated to the cGel moiety via thioether link. Successful KRAS_{G12C} knockdown confirmed that cGel enabled endosomal escape of siRNA after receptor-mediated endocytosis. Western blot analysis showed downregulation of relevant proteins downstream of the RAS pathway and PI3K pathway. Also, toxicity analysis revealed sensitization of cells to Gefitinib after KRAS oncogene knockdown. The receptor binding affinity of Conjugate-1 (CTB–cGel complex) and Conjugate-2 (CTB–cGel–siRNA) using SPR analysis postconjugation was comparable to that of CTB. We believe this system provides a promising and scalable platform technology for gene therapy.

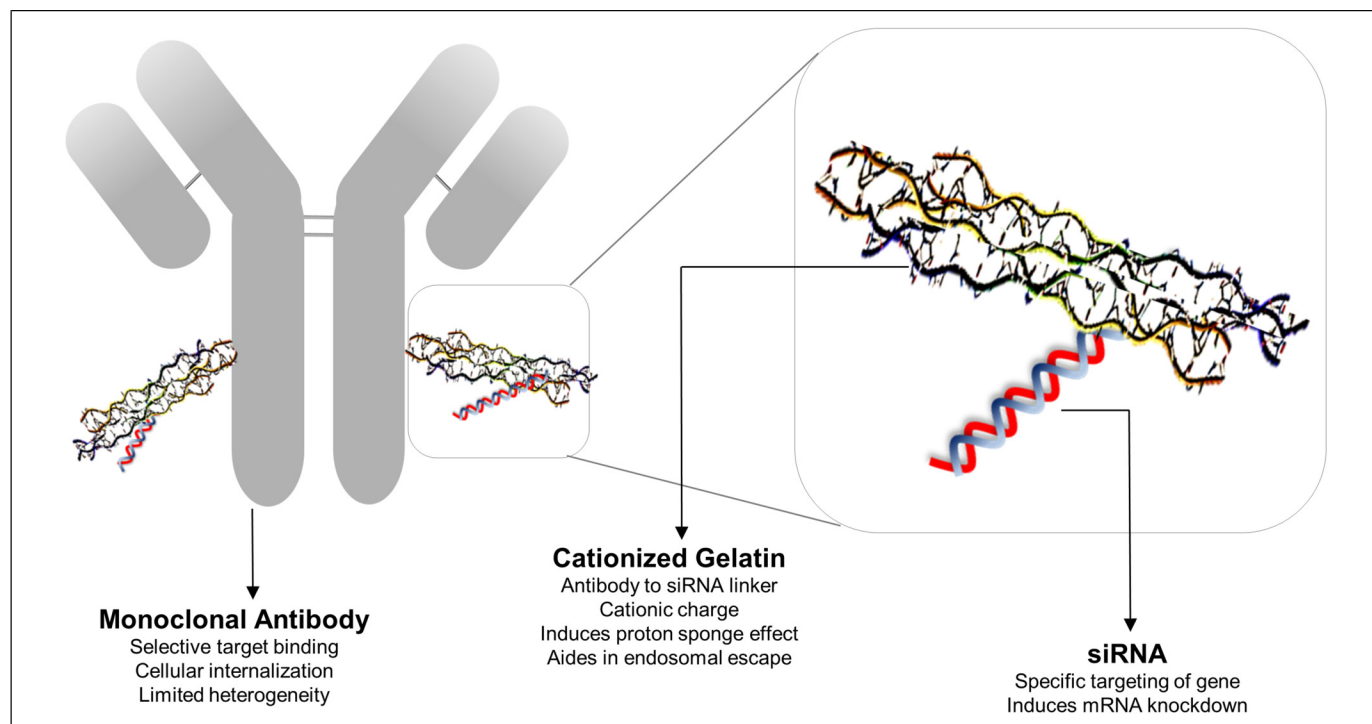


Figure 1. Schematic representation of antibody-cGel-siRNA conjugate and details of their respective functions for targeted siRNA delivery. Abbreviation: siRNA, small-interfering RNA.

Materials and Methods

Materials

Gelatin Type A bloom-110 was purchased from MP Biomedicals (Cat # 960317). *N*-(3-Dimethylaminopropyl)-*N'*-Ethylcarbodiimide Hydrochloride (EDC, Cat # E7750), *N*-Hydroxysuccinimide (NHS, Cat # 130672), Thiazolyl Blue Tetrazolium Bromide (MTT, Cat # M5655), Ethylenediamine (EDA, Cat # 41008) were purchased from Sigma Aldrich. RPMI 1640 media (Cat # AL162S) were purchased from Himedia. Antibiotics, 100X concentrate, for cell culture was purchased from Gibco (Cat # 15140-122). CTB (Erbix) Erbitux 5 mg/mL was procured from Merck. ESHMUNO A resin was purchased from Millipore (Cat # 120089). Protein Assay Dye Reagent Concentrate was purchased from bio-rad (Cat # 5000002). β -Actin (Cat # 8457S), rabbit monoclonal pMEK 1/2 (S221, Cat # 9154S), rabbit monoclonal MEK 1/2 (D1A5, Cat # 8727S), rabbit monoclonal AKT (Cat # 4691S), and rabbit monoclonal pAKT (T308, Cat # 4060S) were purchased from Cell Signalling Technologies. H23 and A549 cell lines were procured from ATCC, USA. Rabbit polyclonal antibody against KRAS (Cat # ab180772) and secondary anti-rabbit IgG-HRP (Cat # ab6721) were purchased from Abcam. Three-color broad range pre-stained protein ladder used for Western Blot analysis was procured from Puregene (Cat # PG-PMT2962). Gt F(ab')₂ Anti-human IgG Y FITC conjugate secondary antibody was procured from Life Technologies (Cat # H10101C). Recombinant human EGFR (rhEGFR)

used for SPR was purchased from Sino Biologicals (Cat # 10001-H08H). Guide-it Complete sgRNA screening system for CRISPR studies was procured from Takara Bio (Cat # 632636).

Cationization of Gelatin

Cationization of gelatin was carried out through activation of carboxyl groups present in the gelatin using EDA. Briefly, 1 g of Type-A Gelatin (bloom 110) was dissolved in 40 mL of DI water. Two hundred and fifty milligrams of EDC and 160 mg of NHS each dissolved in 5 mL of 0.1 M MES/0.5 M NaCl buffer at pH 4.5 were added to the gelatin solution for carboxyl activation. Subsequently, 85 μ l containing 75 mg of EDA was added to the activated gelatin solution and pH was adjusted to 5.25 ± 0.25 using 5 N HCl. The reaction was allowed to continue overnight at 37°C under constant shaking to obtain crude cationized gelatin. For removal of excess EDA, EDC, and NHS, the crude cationized gelatin was purified by desolvation method using acetone precipitation. In the desolvation process, 150 mL of acetone was added to 50 mL of crude cationized gelatin that resulted in the precipitation of gelatin. The pellet was washed with acetone and aspirated. The residual acetone present in the pellet was removed under low pressure using vacuum evaporator (Eppendorf; Speedvac). The purified cationized gelatin (cGel) precipitate was reconstituted in 50 mL of DI water to obtain cGel solution and stored at 4 °C until further usage. The cationization of gelatin was confirmed using zeta-potential measurement.

Synthesis of Conjugate-1

For Conjugate-1 preparation, 10 mL of cGel solution containing 200 mg of cGel was thawed to room temperature and precipitated using acetone in a process as described in the Cationization of Gelatin section. The pellet was dissolved in 8 mL of DMSO for 15 min at 50 °C. Carboxyl activation for preparation of amine-reactive cGel succinimide ester was carried out by adding 100 mg of EDC and 60 mg of NHS dissolved in 2 mL of DMSO. Activation of carboxyl functional groups present in cGel was carried out at a final concentration of 20 mg/mL at 37 °C for 1 h (200 mg of cGel in 10 mL solution). 20 mM BME was used to deactivate the EDC present in the reaction mixture. Subsequently, 40 mg of activated amine-reactive cGel succinimide ester (~25 kDa) was slowly added to 20 mg of purified CTB (5 mg/mL, 150 kDa). The pH of the reaction was maintained between 8.5 and 9 using 1 N NaOH during the cGel addition. The conjugation reaction was allowed to proceed at 37 °C for 2 h and then incubated at 4 °C overnight with gentle shaking to obtain crude Conjugate-1. Subsequently, the reaction mixture was centrifuged at 10 000g for 15 min to remove suspended, undissolved aggregates and particles. The supernatant, containing crude Conjugate-1, was diluted (5-fold) using a buffer containing 10 mM PB, 10 mM NaCl, and 0.1 mM EDTA (pH 7.2). The diluted reaction mixture was then purified using protein-A chromatography as described in the Protein-A Chromatography section. The dilution was essential to reduce the concentration of cGel present in the reaction mixture to avoid resin loading issues during chromatography. The conjugation of cGel to CTB and the removal of reaction impurities were confirmed using RP-HPLC and SDS-PAGE analysis.

Synthesis of Conjugate-2

siRNA sequences 5'-(S-S)-GUUGGAGCUUGUGGCGUAGUU-3' (sense) and 5'-CUACGCCACAAGCUCCAACUU-3' (anti-sense) for KRAS G12C mutation were designed and purchased from GE Dharmacon (Horizon Discovery). Purified Conjugate-1 obtained from Protein-A chromatography was buffer exchanged with 50 mM PBS pH 7.2 and concentrated to 15 mg/mL using ultrafiltration (50 kDa TFF minimize capsule with omega membrane, Pall). siRNA was chemically bound to Conjugate-1 using sulfo-MBS. Sulfo-MBS (4.16 mg) was dissolved in 1 mL PBS. One hundred microliter of Sulfo-MBS solution was then added to Conjugate-1 (15 mg, 1 mL) at pH 7.2 and incubated at room temperature for 30 min. The activated Conjugate-1 was desalted using 50 kDa filter (Amicon) to remove excess sulfo-MBS. The desalting was carried out 3 times for maximum removal of sulfo-MBS. No significant loss of protein was observed in the permeate and the recovery of MBS-Conjugate-1 was ~95% based on RP-HPLC assay. The thiol functionalized siRNA (s-s-siRNA) was reduced as per the manufacturer's instruction and added to MBS-Conjugate-1 at various mole ratios of siRNA:Conjugate-1 (1:1, 2:1, 4:1, and 8:1). The reaction was allowed to proceed at 4 °C overnight with gentle shaking to obtain Conjugate-2. The

loading efficiency was analyzed using gel retardation assay. The molecule was used for various analysis and functional assays without any further processing.

Protein-A Chromatography

CTB and Conjugate-1 reaction samples were purified using Protein-A affinity chromatography to remove impurities such as excipients, excess cGel, EDC, NHS, BME, and salts. Briefly, buffer containing 10 mM PBS, 10 mM NaCl, and 0.1 mM EDTA pH 7.2 was used for equilibrating and washing the resin. Two milliliters of resin volume, having protein binding capacity of 20 mg/mL, were used. Equilibration of the resin was stopped once pH of the resin reached 7.0 to 7.2 and UV absorption reached asymptotic lower levels forming the baseline. Then, respective compounds, ie, CTB (25 mg) and Conjugate-1 (20 mg, based on CTB content in Conjugate-1), were loaded at a flowrate of 100 cm/h. Subsequently, the resin was washed with equilibration buffer for 20 column volumes (40 mL) in case of Conjugate-1 to remove excess cGel and, 5 column volumes (10 mL) in case of CTB. After washing, elution was carried out with 10 mM PBS/H₃PO₄ (pH 2.5). Elution was collected and the pH of the eluate was adjusted to 7.5 with 1 M NaOH. The chromatography was performed using Bio-Rad NGC MPLC system containing inline monitoring system for volume, pH, conductivity, and UV. The concentration of the eluate was estimated using RP-HPLC assay with commercial CTB as the reference standard (5 mg/mL, diluted to 1 mg/mL in PB buffer).

RP-HPLC Analysis

Shimadzu Prominence-I LC-203 °C Plus chromatography system was used for performing RP-HPLC analysis. The analysis was performed with Agilent Xbridge BEH300 C4 column with 3.5 µm particle size for separation. The mobile phase comprised of two buffers, namely solvent A comprising of 0.1% TFA in water and solvent B comprising of 0.1% TFA in acetonitrile. The mobile phase gradient is as follows: (time, % solvent B): 0,20%; 1,20%; 13,45%; 15,80%; 17,20%; 20,20%; the flow rate was 0.5 mL/min and the column temperature was maintained at 80 °C. The chromatograms were obtained at 280 and 214 nm. Ten microliter samples were injected for all analysis. Prior to analysis of the molecules, the developed HPLC method was validated for linearity, specificity, and accuracy using CTB as the reference standard. All analyses were carried out in triplicates with appropriate bracketing standards.

Zeta Potential (ζ)

Zeta potential estimation was performed using Malvern Zeta Sizer (Nano-ZS) instrument. All samples were prepared at a concentration of 1 mg/mL. One milliliter of sample was used for measuring the zeta potential with dip cell kit. The samples were filtered through 0.22 µm PES filters prior to analysis. All analyses were carried out in triplicates.

Gel Electrophoresis

SDS-PAGE analysis was carried out using 12% polyacrylamide gel for analyzing the molecular weight and band shift postconjugation. Ten micrograms of samples namely, CTB, conjugate-1 reaction sample, flow-through/wash of conjugate-1 reaction, and purified conjugate-1 were analyzed under standard reducing and non-reducing conditions.

Agarose gel electrophoresis was carried out for Conjugate-2 samples i.e., siRNA reacted with Conjugate-1 at different mole ratios (1:1, 2:1 and 4:1 of siRNA: CTB), using 1.2% agarose gel to determine the loading capacity. CTB was used as the normalization factor. Five hundred nanograms of conjugate-2 reaction samples were mixed with 5X DNA loading dye and loaded onto the agarose gel. The samples were run in 1X TAE buffer at 100V for 30 min and imaged under UV light.

Native PAGE was used for co-localization analysis. In the co-localization assay, we demonstrated the siRNA to be bound to antibody and existed as one entity. CTB (5 µg), Conjugate-1 (5 µg), and Conjugate-2 (5 µg, 500 ng siRNA) samples were mixed with 5X DNA loading dye and loaded onto 12% native polyacrylamide gel. The gel was run in 1X TAE buffer for 60 min at 100 V. Subsequently, the gel was stained with EtBr and imaged under UV light. The same gel was then stained using Coomassie staining solution to observe the colocalized protein bands. All imaging were performed using Bio-Rad ChemiDoc™ XRS + imaging system.

Fluorescence Microscopy

NCI-H23 cells (0.2 million cells/well) were seeded in a 6-well plate containing glass coverslips and incubated overnight at 37 °C in 5% CO₂. For investigating receptor-mediated endocytosis, the cells were fixed with 4% paraformaldehyde for 10 min. After washing with PBS, coverslips containing the fixed cells were blocked with 1% BSA/ 0.3 M glycine. The excess blocking solution was aspirated and washed with PBS three times. The cells were treated with 1 µM of CTB, Conjugate-1, Conjugate-2, polyclonal IgG, and IgG-cGel for 1 h, and then labeled with secondary antibody (dilution 1:500) for 1 h at room temperature. FITC functionalized anti-human IgG Y was used as the secondary antibody. Prior to fluorescence imaging and analysis, the cells were washed 3 times with PBS to remove non-specific binding of the molecules to cover slips, counter stained with DAPI and mounted onto glass slides. For siRNA internalization analysis, the seeded cells were first treated with 0.1 µM conjugate-2_{FITC} (FITC functionalized siRNA) and 100 pmol of lipofectamine-transfected siRNA_{FITC} for 6 h. Subsequently, the cells were fixed, counter stained with DAPI and mounted onto glass slides before fluorescence imaging.

Surface Plasmon Resonance

GE Biacore T200 was used for the determination of binding kinetics for various molecules. CM5 sensor chip containing carboxymethylated dextran matrix was used for covalent

immobilization of anti-His antibody as per the manufacturer's instructions. Histidine-tagged EGFR (0.25 µg/mL) was then bound to anti-his antibody functionalized CM5 chip at 25 °C. Subsequently, CTB, Conjugate-1, Conjugate-2, IgG, and IgG-cGel at a constant flow rate of 30 µl/min were passed through the chip at various concentrations (3.125, 6.25, 12.5, 25, and 50 nM). 1:1 binding model was used for calculating the association constant (k_a) and dissociation constant (k_d) values. In the model, two criteria were specified, namely (i) kinetic constants to be uniquely determined and (ii) no significant bulk contributions. The model enabled the utilization of the appropriate concentration range for ligand binding affinity analysis for curve-fitting purposes. Using k_a and k_d , the equilibrium dissociation constant, K_D was calculated, and the values of the conjugates were compared to that of CTB reference standard.

Western Blotting

Western blot analysis was carried out by seeding NCI-H23 cells at a density of 0.5 million cells per well in a 6-well plate and incubated at 37 °C. The cells were treated with 50 pmol of transfected siRNA (siTA), 50 nM Conjugate-1, and 50 nM Conjugate-2 (Containing 50 pmol siRNA, 1:1 mole ratio of Conjugate-2: siRNA). siRNA transfection was performed using RNAi Max transfection reagent as per the manufacturer's instruction. The media containing the compounds were aspirated after 6 h of treatment and replaced with basal RPMI 1640 media. After 72 h, the detached cells were transferred to 1.5 mL tubes and centrifuged for 15 min at 4 °C. Thereafter, the cell pellet was lysed using 100 µl of RIPA buffer containing 1X protease phosphatase inhibitor and was incubated at 4 °C for 30 min to obtain cell lysates. The cell lysate were centrifuged at 10 000g for 30 min at 4 °C and the supernatant was collected for further analysis. Protein concentration from each cell lysate was determined using bicinchoninic acid (BCA) protein assay kit (#71285-3, Novagen). Twenty-five micrograms of total protein were loaded onto 12% SDS-PAGE and transferred to methanol-activated PVDF membrane using Mini-PROTEAN Tetra cell setup at 300 mA for 90 min. The transferred blot was first tagged with primary antibodies namely anti-AKT (1:1000 dilution), anti-pAKT (1:2000 dilution), anti-MEK (1:1000 dilution), anti-pMEK (1:1000 dilution), anti-β-actin (1:2000 dilution), and anti-KRAS (1:1000 dilution) for 1 h. The membrane was washed thrice with 1X PBST and then treated with HRP-linked secondary antibody (1:5000 dilution) for 1 h at room temperature. The blots were developed using BioRad Clarity™ western ECL substrate and visualized using ChemiDoc™ XRS + imaging system. Gene expression levels were quantified by densitometry analysis using Image-J tool. The knockdown gene expression study was performed 3 times for validation of KRAS gene knockdown. A similar procedure was followed for A549 lung adenocarcinoma cells.

In Vitro Toxicity Assay

NCI-H23 cells in RPMI 1640 media supplemented with 4.5 g/L D-glucose, 10 mM HEPES, 1 mM sodium pyruvate, 1.5 g/L

sodium bicarbonate, 2 mM L-glutamine, 10% heat-inactivated fetal bovine serum, and 1X penicillin streptomycin were seeded at a density of 10 000 cells per well in 96-well plate and incubated overnight at 37 °C. For determination of cytotoxicity of the molecules, the cells were treated with 5 pmol of siRNA (siTA) that served as the positive control, 5 nM Conjugate-1, 5 nM Conjugate-2 containing 5 pmol of siRNA, and 5 nM CTB that served as the negative control. The treatment was carried out for 72 h. Subsequently, the cells were treated with different concentrations of 100 µl gefitinib (1, 5, 25, 50, and 100 µM) solution for 24 h. The cells were then subjected to 10 µl of 5 mg/mL MTT dissolved in 1X PBS for 4 h. The formazan crystals were solubilized in 100 µl solubilizing buffer and the intensity of the developed color was quantified using spectrophotometer (Biotek Synergy H1) at 570 nm. All analyses were carried out in triplicates.

Crispr-Cas9 Knockout Studies

KRAS exon 2 target from NCI-H23 cells was amplified using forward primer—5' AATATTGTTCTTCTTTGCCTCAGTG 3' and reverse primer—5' TGACATACTCCCAAGGAAAG TAAAG 3' for CRISPR-Cas9 cleavage. Four different sgRNAs targeting exon 2 region in KRAS gene were designed using Chop Chop analysis tool. For sgRNA screening, ribonucleoprotein (RNP) complex was prepared by adding 50 ng of sgRNA to 0.5 µl of Cas 9. The mixture was incubated for 5 min at 37 °C. Thereafter, the sgRNA-Cas9 RNP complex was added to 250 ng of template dsDNA. The cleavage reaction was allowed to proceed for 60 min at 37 °C. Cleavage products were analyzed using agarose gel electrophoresis. The sgRNA with maximum cleavage efficiency was selected for knockout studies. In vitro transcription and screening of the sgRNAs yielded 5' CTGAATTAGCTGTATCGTCAAGG 3' sequence for efficient knockout of KRAS gene. The selected sgRNA was cloned into pGuide-it-tdTomato linear vector. Five micrograms of cloned plasmid were transfected into NCI-H23 cells using X-fect transfection reagent as per the manufacturer's protocol. Fluorescence microscopy was used to confirm the internalization and expression of CRISPR-Cas9 system using RFP expression. Western blot was carried out for 25 µg of the cell lysate to confirm KRAS gene knockout as per details prescribed in the Western Blotting section. For cytotoxicity assay, a similar knockout protocol was performed in 96-well plate containing 10 000 cells and subsequent analysis was performed per the procedure detailed in the In Vitro Toxicity Assay section.

Results

Preparation and Characterization of Conjugate-1

Preparation of the GADS molecule comprises two main steps, namely (i) conjugation of cGel to CTB carried out using the amide linkage to form Conjugate-1 and (ii) conjugation of siRNA to cGel moiety of Conjugate-1 through thioether link to form Conjugate-2, as shown in Figure 2A. Gelatin was

cationized to increase its inherent positive charge prior to the synthesis of Conjugate-1. It is known that the attribute of high positive charge or negative-to-positive charge reversal is required to induce proton sponge effect for the effective endosomal escape of molecules.^{31,32} Also, gelatin has been widely used in pharmaceutical applications including drug delivery and plasmid transfections in several works.³³⁻³⁵ In this work, cationization of gelatin was carried out as per the procedure reported earlier, with few modifications.³³ For instance, instead of dialysis as reported in the earlier work, we removed excess EDA by two-step desolvation method to obtain pure cGel.³⁶ An increase in zeta potential to ~+0 mV from +5 mV indicated successful cationization. Parallely, commercial CTB was purified using Protein-A chromatography to remove formulation components that could interfere during the conjugation procedure. During the conjugation reaction of activated cGel to CTB, the pH drastically dropped from 9 to 6. Since coupling of amine with reactive ester occurs at basic pH, stepwise addition of activated cGel to CTB to maintain the pH between 8.5 and 9 for effective conjugation was warranted.

To determine if the conjugation was successful, SDS-PAGE was performed to observe band shift (Figure 3A). As shown in Figure 3A, upward band shift was observed in the case of reducing gel indicating increased molecular weight due to the addition of cGel to CTB. Multiple bands indicate heterogeneity in the number of gelatin present per antibody. However, this is a common phenomenon in case of ADCs wherein there is a general heterogeneity in the number of drugs attached and the antibody sites wherein the drug is attached. For instance, clinically approved trastuzumab-emtansine ADC has an average drug to antibody ratio of 3.5 and the drug load distribution varies from 0 to 8.³⁷

Interestingly, no upward band shift was observed in the case of non-reducing gel (Figure 3B). On the contrary, a smearing pattern was observed along with a downward band shift of Conjugate-1. To understand this phenomenon, we generated a physical mixture of CTB and cGel. We then purified the mixture using Protein-A chromatography. Upon analyzing the mixture before and after purification with non-reducing SDS-PAGE, we observed that, in the presence of cGel, CTB tends to be "dragged down." However, after purification, ie removal of cGel from the physical mixture, restoration of CTB's band position occurs, as shown in Figure 3B. In the case of Conjugate-1, the smearing pattern is observed postpurification as well, albeit only above the primary band, suggesting excess cGel has been removed during the purification. Based on these results and on comparison of the gel assays of physical mixture, Conjugate-1 reaction and purified Conjugate-1, it can be concluded that cGel is chemically bound to CTB causing the "drag-down" effect to persist. A possible explanation for the artifact "drag-down" effect can be attributed to the molecular nature of gelatin since gelatin does not appear as a distinct band in SDS-PAGE. The conjugation was also monitored using RP-HPLC and the resulting conjugate caused RT shift with a relative retention time (RRT) of 1.1

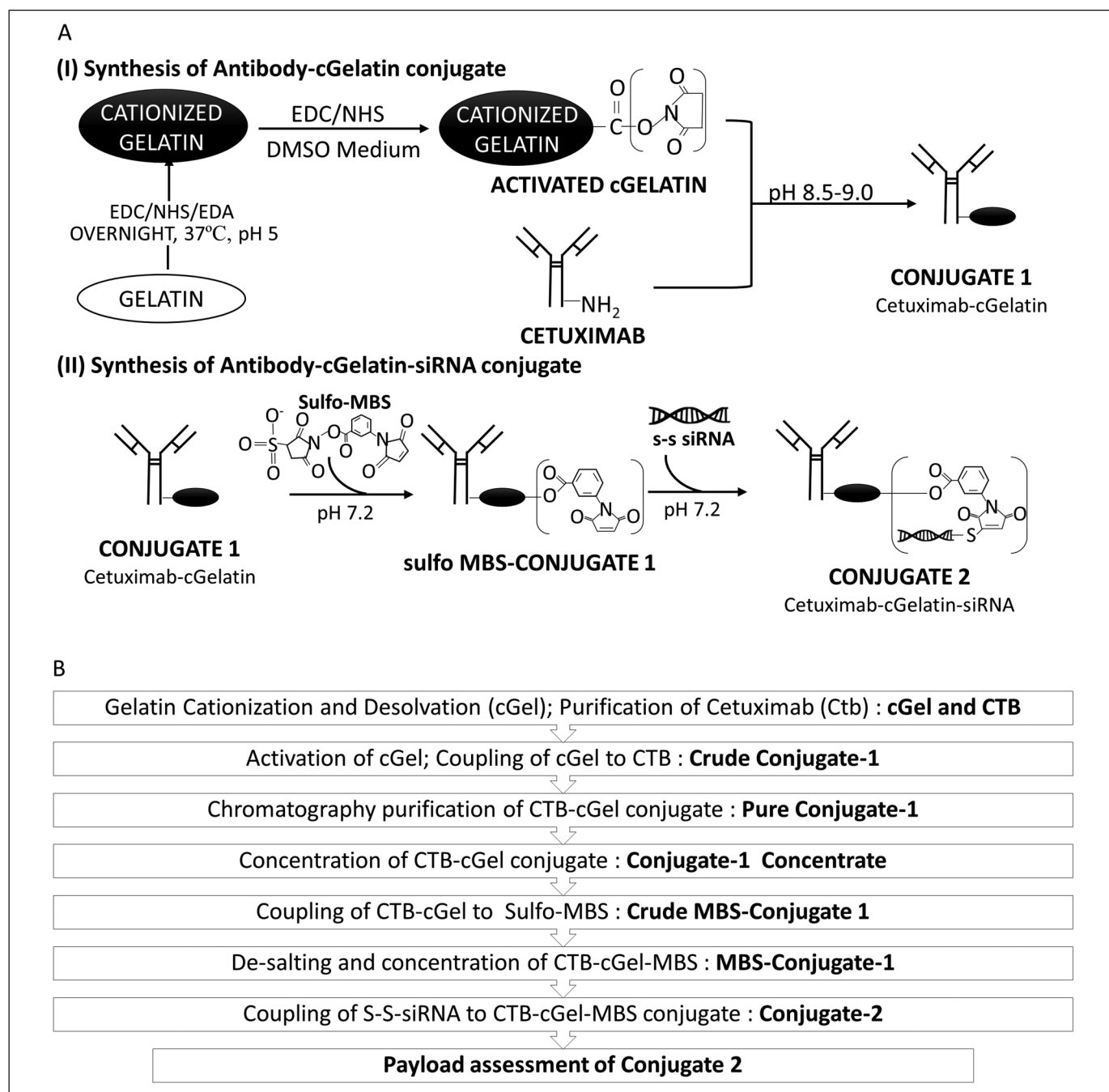


Figure 2. Synthesis of CTB-cGel-siRNA conjugate. (A) Chemistry scheme of gelatin cationization followed by activation of cationized gelatin and conjugation to purified CTB. Purified CTB-cGel (Conjugate-1) is then converted to thiol-reactive maleimide ester and thiol functionalized siRNA is chemically conjugated to form CTB-cGel-siRNA (Conjugate-2). (B) Stepwise unit operation protocol for synthesizing Conjugate-2. Note that the flowchart is applicable for generating other ARCs as well comprising of different antibody and different siRNA sequence. Abbreviations: CTB, cetuximab; siRNA, small-interfering RNA, antibody-siRNA conjugate.

(Figure 3C). Figure 3C shows crude Conjugate-1, unreacted cGel and other impurities. Figure 3D shows the overlay of CTB and purified Conjugate-1 wherein the removal of unreacted cGel was confirmed. From the chromatogram, it can also be observed that peak broadening occurs possibly indicating multiple variants of Conjugate-1 are present in the reaction mixture. In addition, size exclusion chromatography

coupled multiangle light scattering (SEC-MALS) analysis revealed an average of ~ 4 gelatin molecules per CTB molecule (Supplement 1). To ensure the Conjugate-1 can cause proton sponge effect for endosomal escape, charge reversal property was determined using zeta potential. The zeta potential at pH 7 was neutral while the zeta potential increased to $\sim +10$ mV at pH 5 suggesting the molecule carries the required property

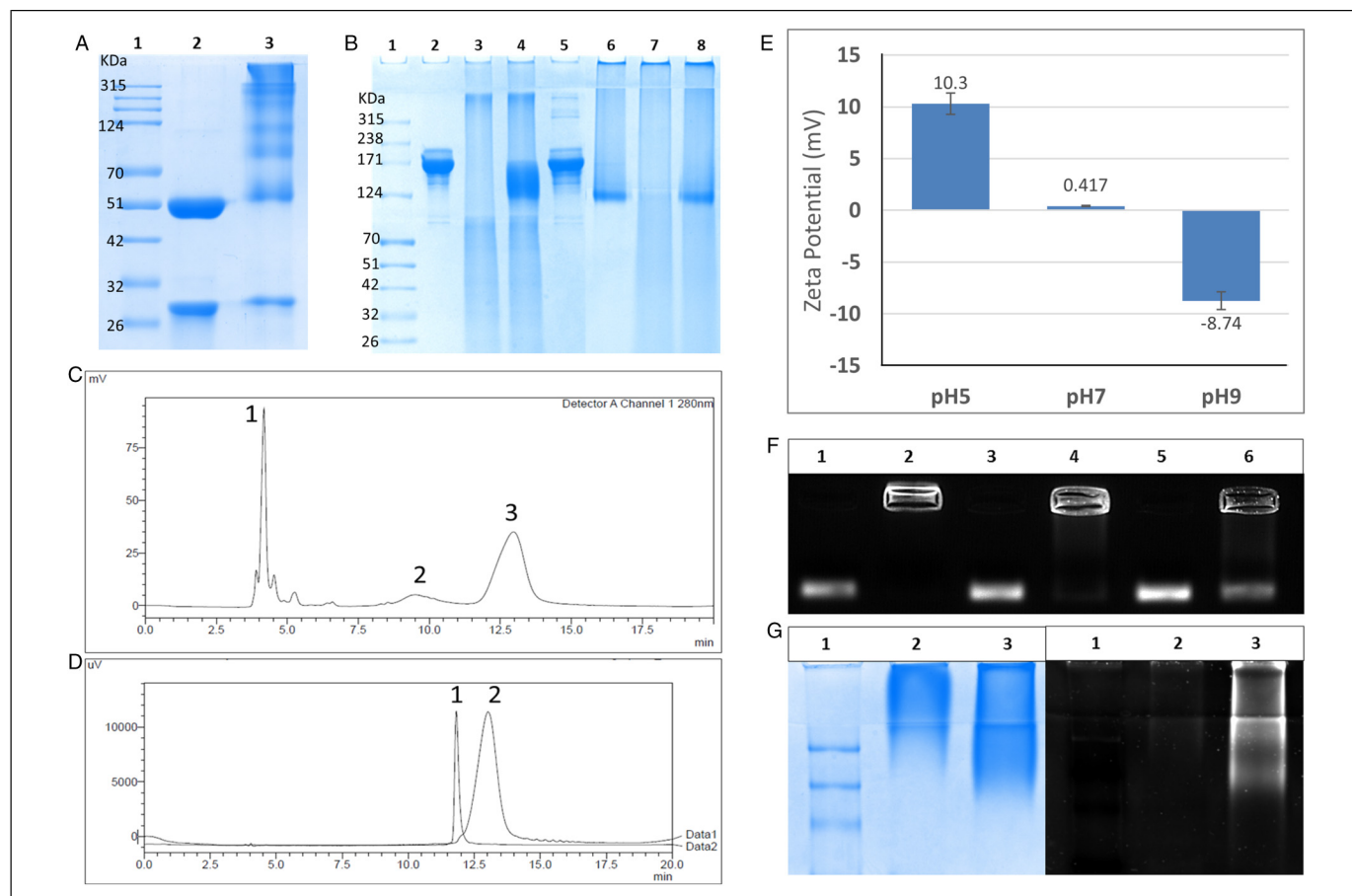


Figure 3. Physicochemical characterization of Conjugate-1 and Conjugate-2. (A) Band-shift assay using reducing SDS-PAGE. Lanes—1: protein marker, 2: CTB, 3: Conjugate-1. (B) Band-shift assay using non-reducing SDS-PAGE. Lanes—1: protein marker, 2: purified CTB from CTB-cGel physical mixture, 3: flow-through of CTB-cGel physical mixture containing cGel, 4: CTB-cGel physical mixture before purification, 5: CTB standard, 6: purified Conjugate-1, 7: flow-through of Conjugate-1 containing free unreacted cGel, 8: crude Conjugate-1 reaction sample. Note that in Lane 5, the smearing pattern is observed as Conjugate 1 is dragged down. However, below Conjugate-1, no residual cGel is observed. (C) RP-HPLC chromatogram of Conjugate-1 reaction sample containing 1: salts such as EDC/NHS, 2: free unreacted cGel and 3: Conjugate-1. (D) Overlay RP-HPLC chromatogram of 1: CTB standard and 2: purified Conjugate-1. (E) Zeta potential measurement of Conjugate-1 at various pH. Charge of Conjugate-1 reverses from negative at basic pH to neutral at pH 7 and positive at acidic pH. (F) Agarose gel electrophoresis for assessing the maximum loading efficiency containing various mole ratios of siRNA: Conjugate-1. Normalization is carried out using CTB concentration assessed using RP-HPLC. Lanes—1: siRNA standard corresponding to 1:1 (siRNA:CTB), 2: Conjugate-2 containing 1:1 (siRNA:CTB), 3: siRNA standard corresponding to 2:1 (siRNA:CTB), 4: Conjugate-2 containing 2:1 (siRNA:CTB), 5: siRNA standard corresponding to 4:1 (siRNA:CTB), 6: Conjugate-2 containing 4:1 (siRNA:CTB). (G) Co-localization assay using concomitant staining of siRNA and protein with EtBr (right) and Coomassie (left), respectively, to show that siRNA is bound to Conjugate-1. Lanes, 1: Protein marker, 2: Conjugate-1 and 3: Conjugate-2.

Abbreviations: CTB, cetuximab; siRNA, small-interfering RNA; RP-HPLC, reverse-phase high-pressure liquid chromatography.

for potential endosomal escape through charge reversal (Figure 3E). Also, it is noteworthy to mention that, while there was no site-directed conjugation of cGel to CTB, no significant effect on the EGFR binding properties of CTB, or unwarranted cytotoxicity was observed indicating the functionality of CTB to be intact as detailed in the following sections.

Preparation and Characterization of Conjugate-2

Thiol functional group at 5' sense strand of siRNA was used to conjugate with the amine functional group of cGel present in Conjugate-1 as shown in Figure 2A. In an earlier study

wherein, ARC platform was used to deliver siRNA, a similar approach was deployed. Thioether link-mediated conjugation of protamine to cysteine residues of antibody was carried out and siRNA was electrostatically complexed to the conjugate.³⁸ However, we found that stable loading through electrostatic interaction was ineffective and several parameters such as concentration of the antibody-cGel, amount of antibody-cGel, and buffer components played a crucial limiting role. Hence, in our work, we used thioether link for establishing a stable chemical bond between siRNA and the cGel moiety of Conjugate-1. Herein, NHS ester of sulfo-MBS was conjugated to the amines of cGel moiety present in the Conjugate-1 to form MBS-Conjugate-1.

The binding of siRNA to MBS-Conjugate-1 was confirmed using gel retardation assay. As shown in Figure 3F, siRNA was bound almost completely to the Conjugate-1.

We determined the loading efficiency of siRNA using densitometry. The analysis revealed maximum loading of 2 moles of siRNA per mole of Conjugate-1 was achievable (Figure 3F). Furthermore, with the addition of excess siRNA, gel retardation using agarose gel showed no increase in the bound siRNA levels and an increase in the free residual siRNA. To prove that siRNA is bound chemically to cGel moiety of the conjugate and not through electrostatic complexation, or to the antibody directly, two control reactions were carried out. For the former case, the reaction was carried out in the absence of sulfo-MBS. For the latter, the reaction was carried out in the absence of cGel. No noticeable intensity of bound siRNA was observed, confirming that the siRNA is indeed chemically linked to cGel moiety of Conjugate-1. Furthermore, we used native PAGE to confirm that siRNA was colocalized with Conjugate-1 by first staining the gel with EtBr followed by Coomassie blue staining for identifying the location of nucleic acid and the protein, respectively (Figure 3G).

A similar process of synthesis was followed to generate IgG-cGel-siRNA compound that served as a negative control for various functional assays. The generic protocol for generation of Ab-cGel-siRNA detailing the unit operations and the respective output is shown in Figure 2B.

Fluorescence Microscopy for Receptor-Mediated Endocytosis

After confirmation of siRNA to be chemically bound to Conjugate-1, qualitative investigation of cellular uptake using fluorescence microscopy was carried out (Figure 4). The cells, incubated on cover slips, placed in 6-well plate, were fixed and then treated with CTB, IgG, Conjugate-1, IgG-cGel and Conjugate-2. Labeling of the compound and controls bound to EGFR receptors was carried out with FITC-tagged secondary antibody. Also, to check specificity, IgG and IgG-based conjugates served as negative controls. First, we checked for specificity by treating the cells with IgG and CTB (Figure 4A). Upon labeling with the secondary antibody, no prominent fluorescence was observed in the case of IgG indicating that IgG does not bind to the cell surface receptors as expected (Figure 4A). In the case of CTB, considerable fluorescence was observed (Figure 4A). For Conjugate-1 and Conjugate-2, specific receptor binding was confirmed through uniform fluorescence indicating that modification of antibody with cGel does not inhibit the ligand's ability for receptor-mediated endocytosis. However, non-specific fluorescence was observed for IgG-cGel. A possible reason for non-specific binding could be attributed to the positively charged cationized gelatin present along with IgG that interacts with negatively charged cell surface leading to non-specific binding through electrostatic interaction. To confirm successful lipofection of FITC-tagged siRNA (siRNA_{FITC}), the cells were first

transfected and fixed later. A similar procedure was adopted for Conjugate-2_{FITC} and for CRISPR-Cas9 transfection. Fluorescence was observed in the cells treated with siRNA_{FITC} and Conjugate-2_{FITC} indicating successful internalization (Figure 4B). For IgG-cGel-siRNA_{FITC}, no fluorescence was observed. The fluorescence microscopy data suggest the compound to (i) specifically target EGFR receptors and (ii) undergo internalization through receptor-mediated endocytosis.

SPR Analysis of Ligand Binding Kinetics

Fluorescence microscopy confirmed cellular internalization of the GADS conjugates to be driven predominantly via receptor-mediated endocytosis. However, it was important to determine whether modification of CTB carried out to obtain Conjugate-1 and subsequently, Conjugate-2 affected the binding affinity of the antibody towards EGFR. We used SPR analysis for quantitative determination of steady-state affinity and binding kinetics for various molecules using Biacore T200. CTB, Conjugate-1, Conjugate-2, IgG, and IgG-cGel were analyzed at different concentrations (3.125, 6.25, 12.5, 25, and 50 nM). Nominal reduction in binding affinity with increased K_D value was observed for Conjugate-1 when compared with that of CTB. Using the kinetics model, K_D of CTB was found to be ~ 0.1 nM while that of Conjugate-1 was ~ 0.3 nM. However, no change in K_D was observed for Conjugate-2 vis-à-vis Conjugate-1 suggesting (i) no further modifications occur within the antibody and more importantly, (ii) confirming that siRNA is bound to cGel in Conjugate-2 or at-least, not further affecting the receptor binding affinity of the antibody. IgG did not bind to the functionalized CM5 chip and hence, the kinetics could not be determined for IgG conjugates. Figure 5 shows the kinetics of various molecules and summary of ligand binding kinetic constants.

RAS and Associated Protein Regulation Post-knockdown and Post-knockout

Previous reports have shown that targeting KRAS mutation results in downregulation of phosphorylated RAS downstream proteins —pMEK and pERK as well as PI3K downstream protein pAKT.^{39,40} In this work, to investigate the efficacy of the molecule for specific KRAS_{G12C} knockdown, expression of the key components of RAS pathway and its cascading effect on PI3K pathway was investigated using western blot. H23 cells harboring KRAS_{G12C} mutation were treated with Conjugate-2 along with appropriate positive and negative controls. After 72 h of treatment, the cells were lysed, and the extracted proteins were analyzed for gene expression study using western blot. The results were similar to that of earlier works wherein, downregulation of pMEK and pAKT was observed^{39,40} (Figure 6A). Also, in the case of cells treated with Conjugate-2, almost-complete knockdown of KRAS oncogene was observed. To check for specificity, we treated A549 cells harboring G12S mutation with G12C-specific Conjugate-2 (data not shown). No downregulation in downstream

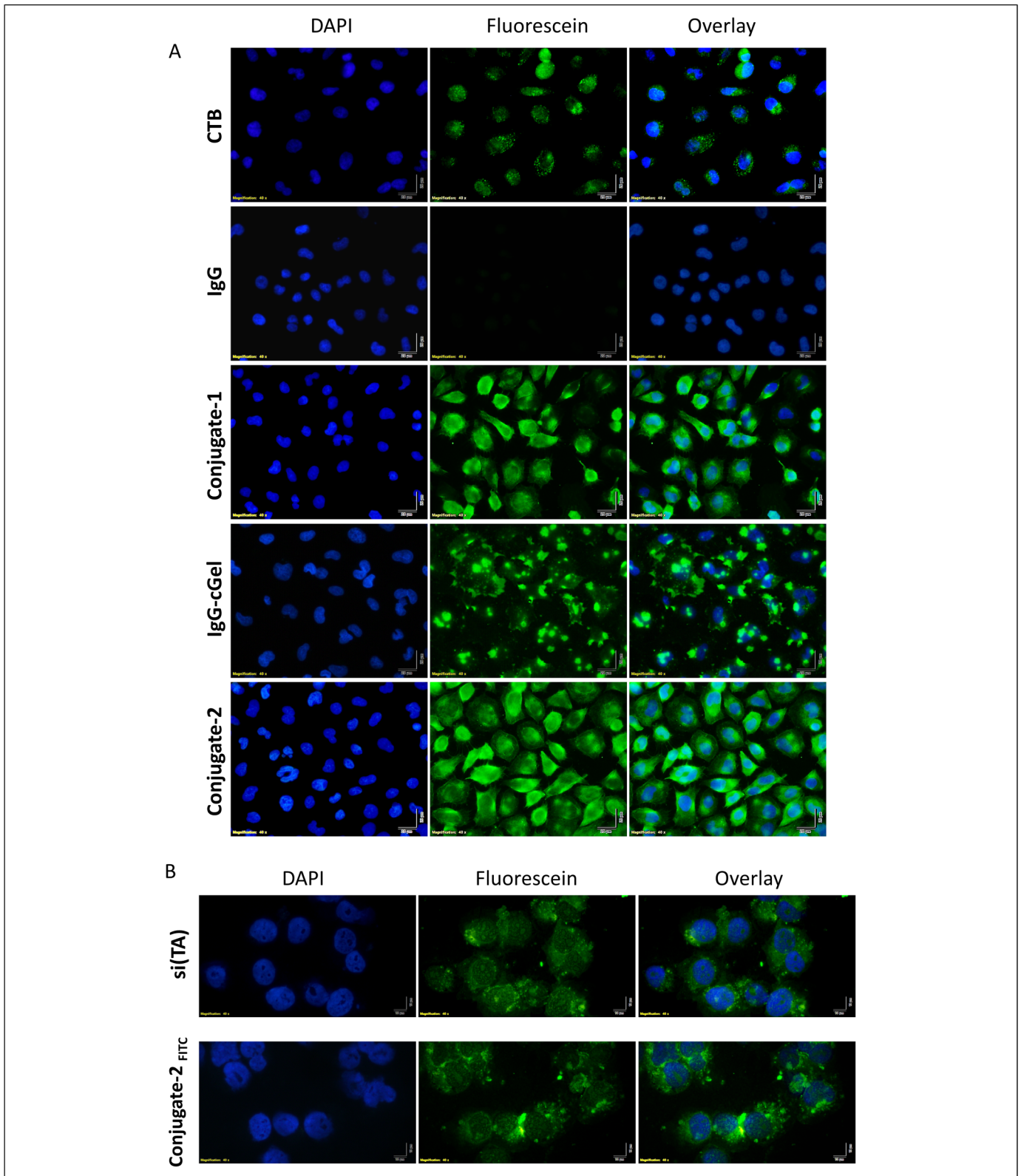


Figure 4. Fluorescence microscopy for assessing receptor-mediated endocytosis and internalization. (A) FITC induced fluorescence after treating the fixed cells with various molecules—CTB, IgG, Conjugate-1, IgG-cGel serving as negative control and Conjugate-2 for assessing the specificity of the molecules and receptor affinity. (B) Internalization assessment using Conjugate-2 containing FITC-labeled siRNA and transfected FITC-labeled siRNA.

Abbreviations: CTB, cetuximab; siRNA, small-interfering RNA.

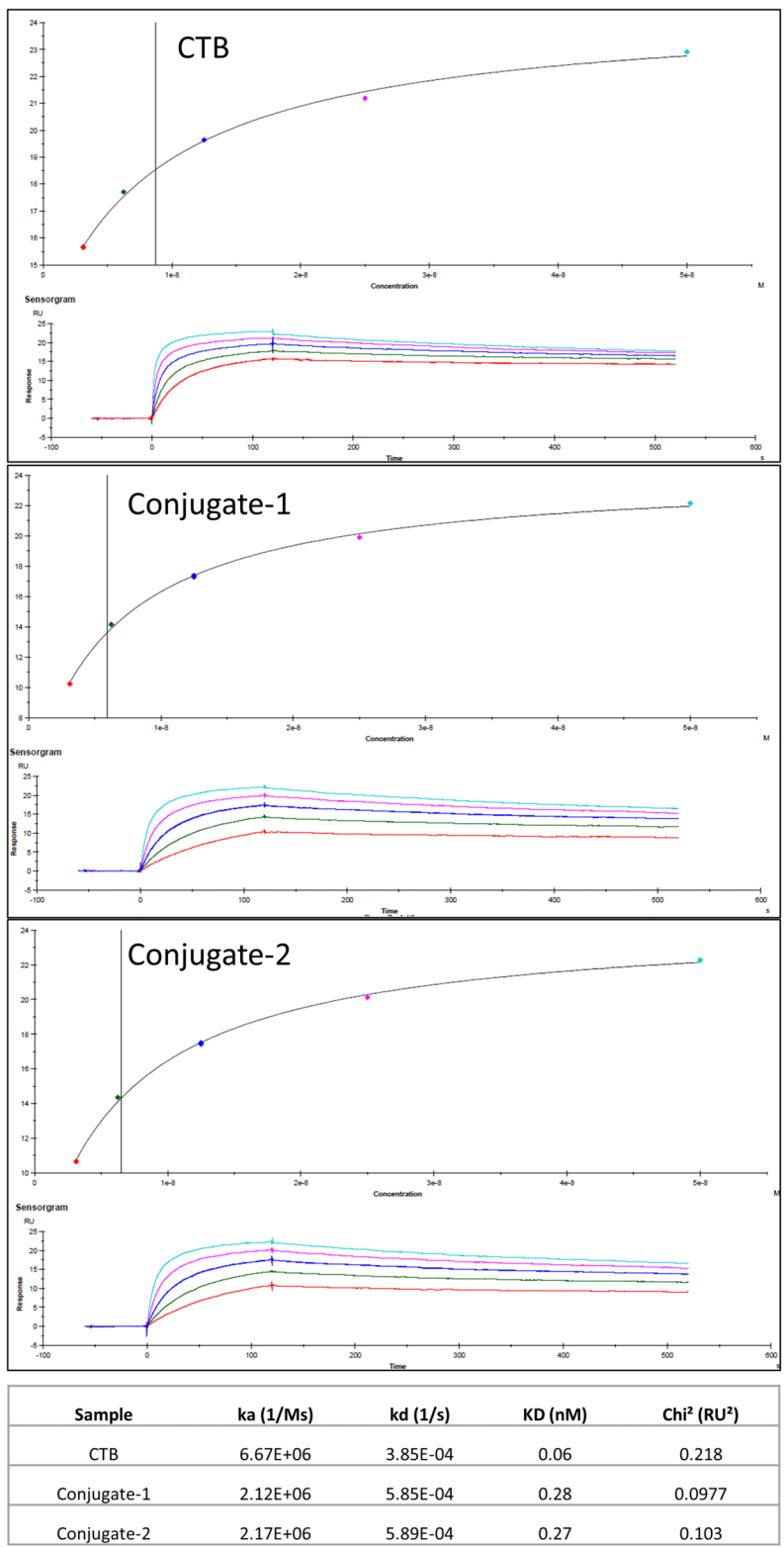


Figure 5. Steady-state affinity (top) and kinetics (bottom) of CTB, Conjugate-1, and Conjugate-2 using SPR analysis carried out in Biacore T200. The table details the k_a , k_d and K_D values of the three conjugates. Abbreviations: CTB, cetuximab; SPR, surface plasmon resonance.

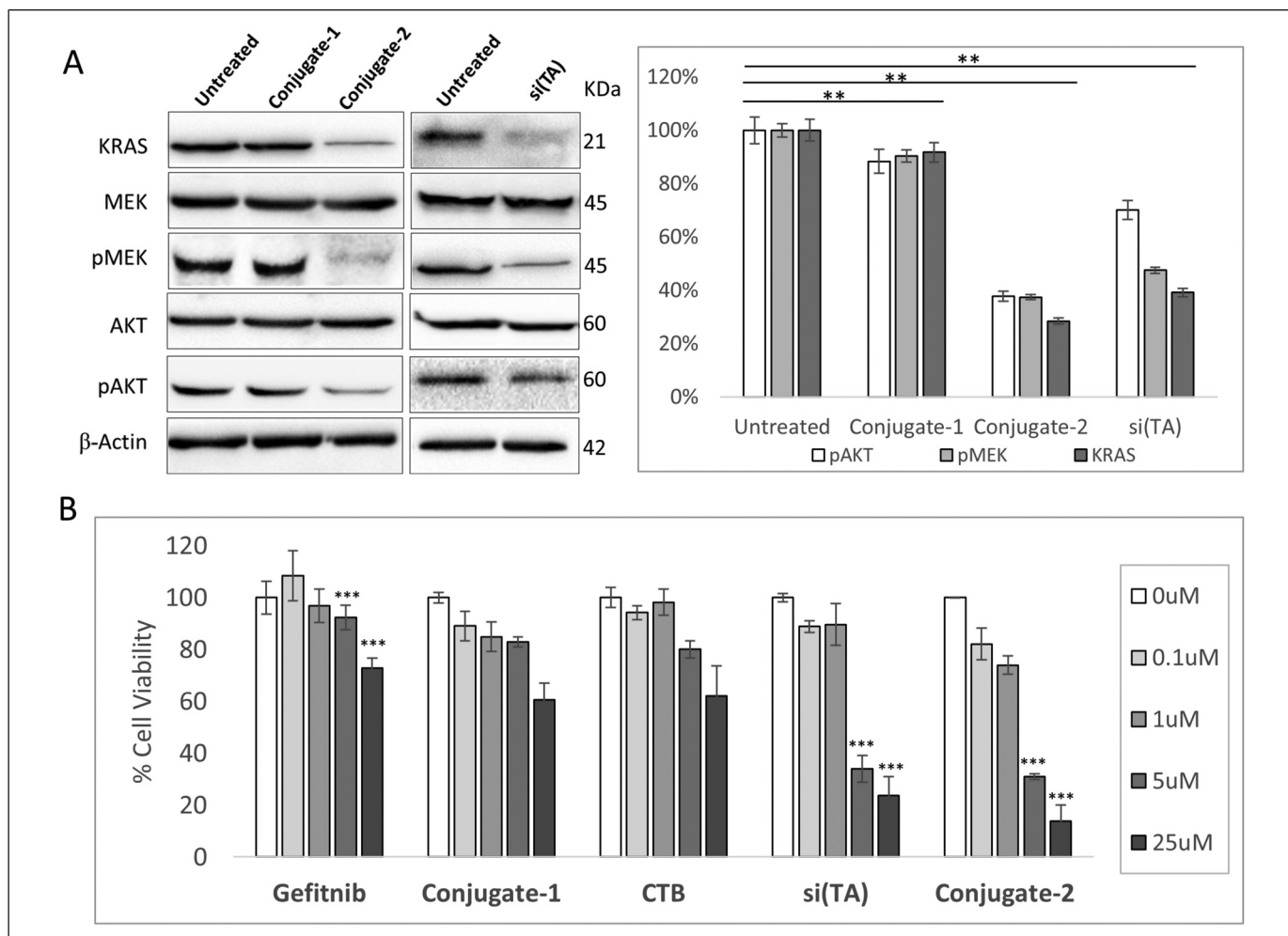


Figure 6. In vitro functional studies. (A) Western blot analysis of H23 cells treated with Cojugate-1, transfected siRNA-si(TA) that serves as positive control and Cojugate-2. Downregulation of KRAS and downstream phosphorylated proteins indicate successful gene knockdown. $**P < .01$ (B) Cell viability assay for H23 cell treated with various molecules and subsequently treated with Gefitinib for assessing knockdown mediated TKI sensitization effect. Loss in viability of cells post gefitinib exposure for Cojugate-2 and si(TA) treated cells indicate sensitization of cells towards the TKI post-knockdown. $***P < .001$.

Abbreviations: siRNA, small-interfering RNA; si(TA), transfected siRNA using lipofectamine; TKI, tyrosine kinase inhibitor.

proteins were observed indicating the molecule to be specific for G12C mutation. Similar to knockdown, knockout of KRAS Exon 2 using CRISPR–Cas9 resulted in almost-complete downregulation of KRAS, pMEK and pAKT (Figure 7A). Prior to knockout, the treated cells were analyzed using fluorescence microscopy after 48 h of transfection. Expression of RFP was observed suggesting successful plasmid internalization (Figure 7B).

Cytotoxicity Assay

After knockdown of KRAS using siRNA and knockout using CRISPR–Cas9, we checked for cytotoxicity using MTT assay and analyzed the cells upon knockdown or knockout. In all cases, 5 pmol of siRNA was used for treatment. The assay revealed no significant loss in the viability of the cells for all the molecules including Cojugate-2 and si(TA). It has been reported earlier that disruption of oncogenic pathways usually

results in altered downstream signaling cascade for cell survival and, not leading to apoptosis in many cases.^{40,41} However, the altered signaling pathway is also known to result in sensitization of the cells to inhibitors.^{42–44} In this work, 72 h post-knockdown, we treated the cells with various concentrations of gefitinib. Approximately 70% loss in cell viability at 5 μ M gefitinib concentration was observed for cells treated with Cojugate-2. The result was similar to that of si(TA)-treated cells which served as the positive control (Figure 6B). These results corroborate the results of earlier studies wherein, targeted knockdown of mRNA sensitized the cells toward TKIs in the case of NSCLC harboring KRAS_{G12C} mutation.^{39,40}

Discussion

Delivery of siRNA using ARC platform is gaining momentum for various cancers and diseases since (i) the platform provides

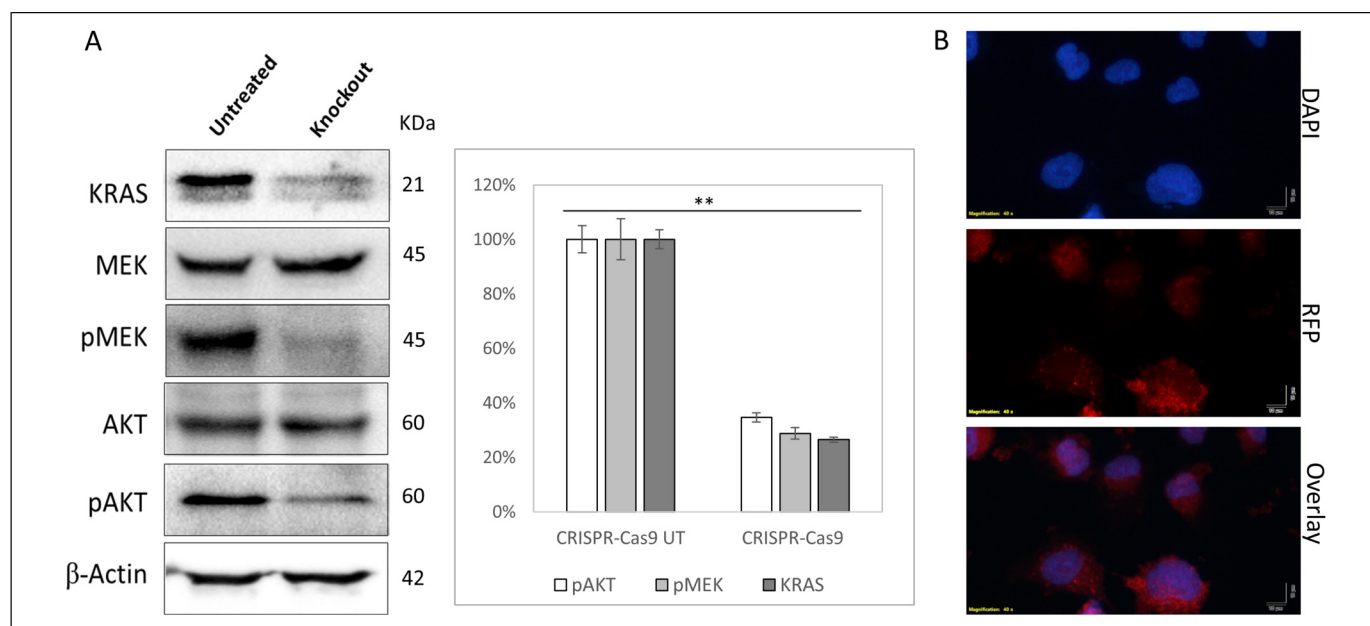


Figure 7. CRISPR–Cas9 knockout analysis of KRAS in NCI-H23 cells. (A) Western blot analysis after knockout of KRAS mutation. Almost-complete knockout is observed for KRAS protein, while downregulation of pMEK and pAKT is observed. $**P < 0.01$. (B) RFP expression in transfected cells indicates successful transfection and gene modification. Abbreviations: CRISPR, clustered regularly interspaced small palindromic repeats.

stable and targeted delivery of siRNA using mAB and (ii) has a higher potential for clinical translation.^{26,45–49} The targeting ligand and siRNA design is fixed depending on the biomarker and the gene sequence, respectively. The emerging interest for siRNA delivery is mostly related to the linker technology to achieve maximum stability, optimal bioavailability, cytoplasmic translocation, and specific knockdown. Most linker technologies are based on small molecules. However, few works have reported macromolecule cationic linker such as protamine for developing efficient ARCs.^{28,38} In this work, we developed a delivery system based on ARC platform, called GADS, with gelatin as the linker between antibody–CTB and KRAS_{G12C}-specific siRNA. Gelatin and gelatin NPs have been routinely used for drug delivery and plasmid transfections.^{33,35,40} While gelatin NPs have been reported for several such delivery systems, no report till date has used gelatin as a linker to our knowledge. For GADS, cationized gelatin as linker enables antibody to carry siRNA, and in addition, provides the property of charge reversal to effect endosomal escape postreceptor-mediated endocytosis. Indeed, using the knockdown results combined with receptor-mediated endocytosis, we hypothesize the mechanism of siRNA release to be mediated via cationic gelatin (Figure 8). CTB moiety of Conjugate-2 targets EGFR receptor enabling cellular internalization. Cationic gelatin assists in proton sponge effect allowing endosomal escape to cytoplasm and releasing the siRNA to interact with RISC complex for effecting mRNA knockdown. The release of siRNA is possibly mediated through various proteinases including gelatinases—MMP-2 and MMP-9 present in cytoplasm by degrading the gelatin. Alternatively, RISC

directly complexes with the antisense strand of siRNA present in the conjugate and enables mRNA knockdown.⁵⁰ However, it is difficult as on date, to detect and predict the precise mechanism of release and siRNA–RISC complexation within the cells for GADS molecule.

Binding of siRNA to Conjugate-1 was carried out through chemical linkage rather than electrostatic complexation. The loading of siRNA through electrostatic interaction onto the carrier molecule requires several optimal parameters such as high N/P ratio, lower moles of carrier molecule, and stable formulations.⁵¹ For instance, electrostatic condensation of siRNA using fatty acid amides of spermine reported N/P ratio of 22 for efficient loading of siRNA.⁵² In our case, the number of moles of carboxyl group (75 mmol/100 g of gelatin) present per mole of gelatin was calculated to be ~ 32 . The asymptotic levels of cationization and conversion of carboxyl group to amines are 50% as reported earlier.³³ Assuming similar levels of cationization, the maximum moles of amines present per mole of gelatin is 16. Based on the theoretical values, we carried out electrostatic complexation at theoretical N/P ratio of 1,2,4 and 8. The maximum binding and saturation was found at N/P ratio of 4 that roughly translated to a very low loading efficiency requiring 4 moles of antibody to carry one mole of siRNA. On the other hand, using sulfo-MBS to chemically conjugate siRNA with cGel moiety, we successfully conjugated 2 moles of S-S-siRNA to 1 mole of Conjugate-1.

It is also important to synthesize ARCs that is scalable. For generating homogenous API, monitoring and estimating the levels of known and unknown impurities is essential. RP-HPLC is widely used for impurity detection and reaction

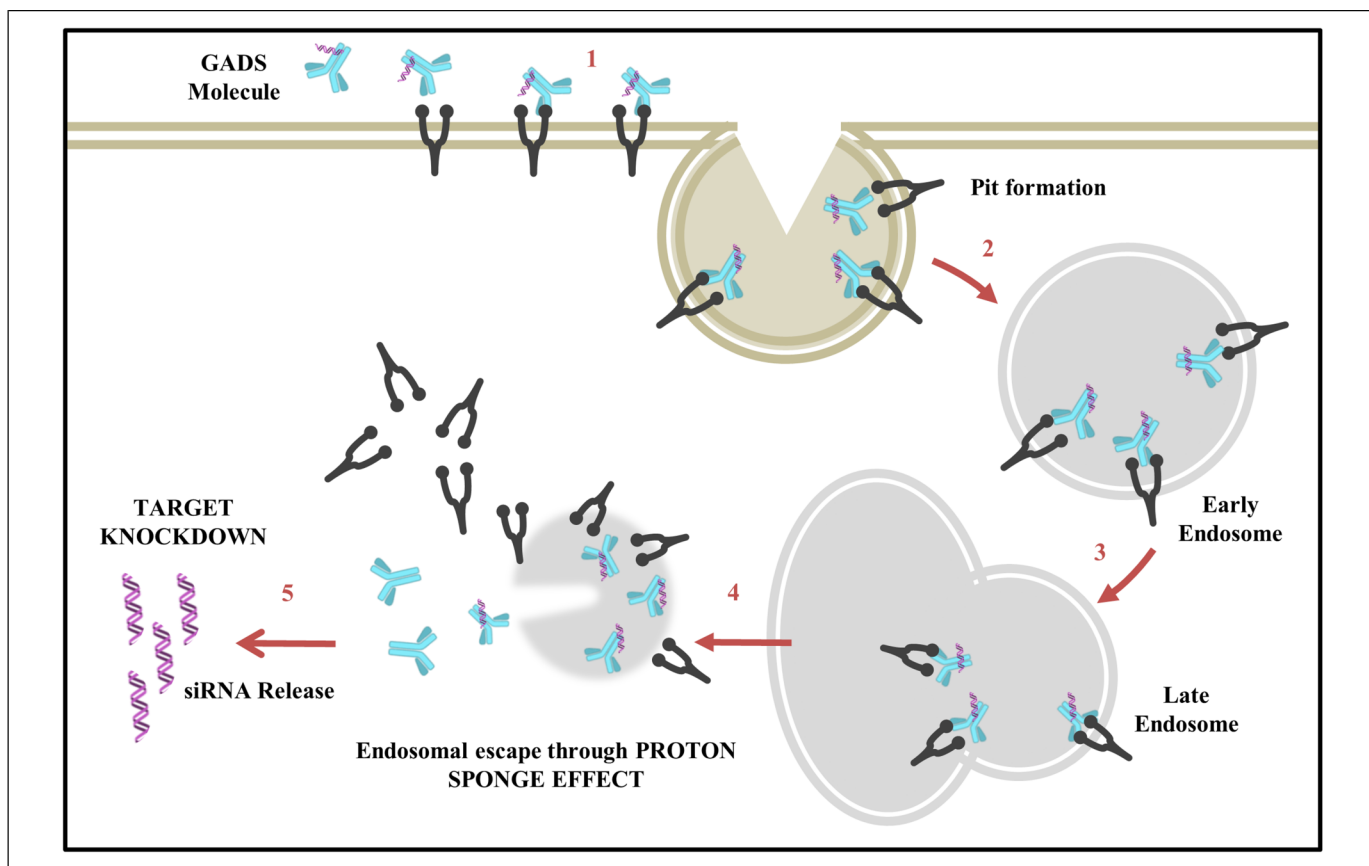


Figure 8. Schematic representation of possible mechanism of action of GADS molecule occurring in 5 stages. In stage 1, the GADS molecule binds to the surface receptor of the cells and is internalized. In stage 2, the molecule enters the endosomes and traverses to late endosome (stage 3). In stage 4, the molecule undergoes endosomal escape and releases siRNA in cytoplasm (stage 5) for RISC complexation and mRNA knockdown. Abbreviations: GADS, gelatin-antibody delivery system; siRNA, small-interfering RNA; RISC, RNA-induced silencing complex.

monitoring. In the case of GADS, the known impurities were the reaction components such as EDC, NHS, Sulfo-MBS among other salts, and unreacted cGel. After establishing the RP-HPLC retention time for various impurities, purification was optimized. One of the important factors was removal of excess cGel. The presence of unreacted cGel in Conjugate-1 impacts the loading efficiency of siRNA since siRNA will not only bind to Conjugate-1 but also with unreacted cGel, thereby reducing loading efficiency. Therefore, after subjecting crude Conjugate-1 to Protein-A column chromatography, 20 column volume washing was essential to remove all unreacted cGel present in the reaction mixture. Similarly, purification of MBS-Conjugate-1 and storing the thiol-reactive compound at appropriate conditions with essential formulation provides a potential scalable platform. Since maleimide-thiol reaction is highly stable and spontaneous, it is hypothesized that purified thiol-reactive antibody-cGel complex can be fill-finished separately and siRNA could be added to the complex prior to dosage. The proposed procedure eliminates stability issues and loss of potency pertaining to siRNA.

After synthesis and characterization of GADS conjugate, we carried out analysis for Conjugate-2 along with appropriate controls, for understanding its functional attributes. It is known that

any chemical modification of antibody can possibly result in decreased ligand binding affinity. Healey et al.⁵³ reported 4-fold decrease in antigen binding affinity for one of their conjugated antibodies vis-à-vis unconjugated antibody. In another work, antibody variants with point mutation(s) were ranked based on HER2 binding affinities for optimal ADC and the K_D values were significantly different for variants differing by even a single amino acid.⁵⁴ To determine if the GADS conjugate was functional with respect to receptor affinity, we carried out SPR analysis and compared the K_D values against CTB. K_D of CTB, Conjugate-1, and Conjugate-2 were ~ 0.06 , ~ 0.28 and ~ 0.27 nM, respectively, which is similar to the K_D values reported for CTB in earlier works.^{55,56} For Conjugate-1, although there is ~ 4.5 -fold decrease in affinity, it is known that K_D values in nanomolar range are considered high affinity antibodies. The decrease can be attributed to cGel addition to the antibody's backbone thereby nominally reducing the affinity. The addition of siRNA to the complex caused no significant change to the K_D value, suggesting no further modification occurs to the antibody backbone. Having established satisfactory ligand affinity, we investigated KRAS knockdown effects on downstream proteins. RAS pathway is governed via Ras/Raf/Mek/Erk pathway.⁵⁷ After treatment of

the cells, significant downregulation of KRAS, pMEK and pAKT were observed for Conjugate-2 and si(TA)-treated cells. No change in the protein expression levels were found for CTB, Conjugate-1, or IgG-cGel-siRNA. Albeit knockdown, there was no significant loss in cell viability. It is known that knockdown or knockout of KRAS causes downregulation of several proteins including pMEK and pERK, leading to alterations in downstream signal cascades by triggering signals for alternate cell survival pathways.^{30,39} Also, multiple levels of crosstalk exist between mitogenic Ras/MAPK pathway and survival PI3K/AKT pathway causing positive or negative feedback depending upon the type of cells.⁵⁸ In this work, downregulation of pAKT upon knockdown of KRAS suggested negative feedback loop conforming to earlier reports.^{39,40} The mechanism of crosstalk in the case of NSCLC cells between KRAS and PI3K pathway was reported earlier to be governed through Shp2.⁴⁰ Indeed, Shp2 has been identified as a critical regulator for response towards TKIs.⁵⁹ Earlier reports also suggest complex association or dissociation between GAB1 and Shp2 affecting the feedback loop between Ras and Akt pathways.^{40,60} Interestingly, TKIs such as gefitinib acts on dysregulated Shp2, inhibiting the alternate survival pathways leading to cellular apoptosis.^{59–61} Since we observed downregulation of pAKT upon knockdown of KRAS, it was of interest to investigate whether the cells are sensitized to gefitinib. Approximately, 70% loss in cell viability was found at 5 μ M gefitinib concentration for cells treated with Conjugate-2 while no loss was observed for standalone gefitinib (5 μ M) or Conjugate-1-treated cells. Interestingly, knockout of KRAS using CRISPR-Cas9 also showed similar protein regulation profiles and no significant loss in viability was observed prior to treatment with gefitinib.

In summary, the combined data of western blot and viability assay reveal Conjugate-2 undergoes cytoplasmic translocation for mRNA knockdown. Furthermore, the conjugate works similar to lipofectamine-transfected siRNA, albeit the delivery of GADS molecule is targeted. Although non-specific binding was observed in fluorescence microscopy for IgG-cGel conjugate, the conjugate can be deemed non-functional. The presence of cGel in the conjugate does not cause non-targeted cellular penetration as observed through toxicity assay. Furthermore, no loss in viability for Conjugate-2 without gefitinib and sensitization towards TKI post-knockdown confirms efficient delivery of Conjugate-2. Correlating all the results, GADS technology shows promising potential as an ARC platform. However, it would be interesting to investigate the effect of GADS platform on whole-genome level. We believe, exhaustive RNA-Seq profiling will further our understanding of the intracellular regulatory aspects and shed light on more effective inhibition strategies.

Conclusion

The GADS technology developed in this study is based on ARC platform for targeted and stable delivery of siRNA. The POC used for demonstrating the technology shows KRAS_{G12C}

knockdown and subsequently, sensitization of NSCLC cells toward small molecule TKI. The CTB component targets over-expressed EGFR of NSCLC cells enabling receptor-mediated endocytosis while the cGel acts as a linker and aides in endosomal escape. The process for generating GADS molecule requires formulation and stability only for thiol-reactive antibody-linker intermediate, since siRNA can be conjugated prior to dosing. In addition, the process is designed for removal of impurities based on existing mAB purification methodology, thereby allowing relatively easier scale-up operations. While significant amount of work is required to enter clinical phase for the technology including formulation development, consistency batches, detailed physicochemical characterization, and in vivo efficacy studies, we believe GADS technology to be a potential ARC platform for gene therapy.

Authors' Contributions

R S hypothesized and conceptualized the study. K S, R S and R R designed the experiments. K S and L S performed the synthesis and characterization of the molecules. K H performed purification and LC-related experiments. All authors contributed equally to analyzing data and writing the manuscript. We are grateful to Levim Biotech LLP and Jatin Vimal for supporting the project, fostering industry-academia collaborations and furthering fundamental research in the field of genetic engineering. We thank Biotechnology Industry Research Assistance Council (BIRAC), India for supporting the project.

Declaration of Conflicting Interests

The authors declared no potential conflicts of interest with respect to the research, authorship, and/or publication of this article.

Funding

This work was funded by Levim Biotech LLP, Chennai, Tamil Nadu, India. The funders had no role in the experimental design, data collection, analysis and preparation of the article.

ORCID iD

R. Srikar  <https://orcid.org/0000-0002-5935-7712>

Supplemental Material

Supplemental material for this article is available online.

References

1. Morgillo F, Della Corte CM, Fasano M, Ciardiello F. Mechanisms of resistance to EGFR-targeted drugs: lung cancer. *ESMO Open*. 2016;1(3):e000060.
2. Stewart EL, Tan SZ, Liu G, Tsao MS. Known and putative mechanisms of resistance to EGFR targeted therapies in NSCLC patients with EGFR mutations—a review. *Transl Lung Cancer Res*. 2015;4(1):67-81.
3. de Castro Carpeno J, Belda-Iniesta C. KRAS mutant NSCLC, a new opportunity for the synthetic lethality therapeutic approach. *Transl Lung Cancer Res*. 2013;2(2):142-151.

4. Whitehead KA, Langer R, Anderson DG. Knocking down barriers: advances in siRNA delivery. *Nat Rev Drug Discov*. 2009;8(2):129-138.
5. Hickerson RP, Vlassov AV, Wang Q, et al. Stability study of unmodified siRNA and relevance to clinical use. *Oligonucleotides*. 2008;18(4):345-354.
6. Shim MS, Kwon YJ. Efficient and targeted delivery of siRNA in vivo. *FEBS J*. 2010;277(23):4814-4827.
7. Guo S, Huang Y, Jiang Q, et al. Enhanced gene delivery and siRNA silencing by gold nanoparticles coated with charge-reversal polyelectrolyte. *ACS Nano*. 2010;4(9):5505-5511.
8. Martino S, di Girolamo I, Tiribuzi R, D'Angelo F, Datti A, Orlacchio A. Efficient siRNA delivery by the cationic liposome DOTAP in human hematopoietic stem cells differentiating into dendritic cells. *J Biomed Biotechnol*. 2009;2009:410260.
9. Sarisozen C, Salzano G, Torchilin VP. Recent advances in siRNA delivery. *Biomol Concepts*. 2015;6(5-6):321-341.
10. Williford JM, Wu J, Ren Y, Archang MM, Leong KW, Mao HQ. Recent advances in nanoparticle-mediated siRNA delivery. *Annu Rev Biomed Eng*. 2014;16:347-370.
11. Morgan E, Wupperfeld D, Morales D, Reich N. Shape matters: gold nanoparticle shape impacts the biological activity of siRNA delivery. *Bioconjug Chem*. 2019;30(3):853-860.
12. Dong Y, Siegwart DJ, Anderson DG. Strategies, design, and chemistry in siRNA delivery systems. *Adv Drug Delivery Rev*. 2019;144:133-147.
13. Kim HJ, Takemoto H, Yi Y, et al. Precise engineering of siRNA delivery vehicles to tumors using polyion complexes and gold nanoparticles. *ACS Nano*. 2014;8(9):8979-8991.
14. Elbakry A, Zaky A, Liebl R, Rachel R, Goepferich A, Breunig M. Layer-by-layer assembled gold nanoparticles for siRNA delivery. *Nano Lett*. 2009;9(5):2059-2064.
15. Song WJ, Du JZ, Sun TM, Zhang PZ, Wang J. Gold nanoparticles capped with polyethyleneimine for enhanced siRNA delivery. *Small*. 2010;6(2):239-246.
16. Patil Y, Panyam J. Polymeric nanoparticles for siRNA delivery and gene silencing. *Int J Pharm*. 2009;367(1-2):195-203.
17. Gary DJ, Puri N, Won YY. Polymer-based siRNA delivery: perspectives on the fundamental and phenomenological distinctions from polymer-based DNA delivery. *J Control Release*. 2007;121(1-2):64-73.
18. Kulkarni A, DeFrees K, Hyun SH, Thompson DH. Pendant polymer:amino-beta-cyclodextrin:siRNA guest:host nanoparticles as efficient vectors for gene silencing. *J Am Chem Soc*. 2012;134(18):7596-7599.
19. Grayson AC, Doody AM, Putnam D. Biophysical and structural characterization of polyethylenimine-mediated siRNA delivery in vitro. *Pharm Res*. 2006;23(8):1868-1876.
20. Li X, Chen Y, Wang M, Ma Y, Xia W, Gu H. A mesoporous silica nanoparticle—PEI—fusogenic peptide system for siRNA delivery in cancer therapy. *Biomaterials*. 2013;34(4):1391-1401.
21. Kanasty R, Dorkin JR, Vegas A, Anderson D. Delivery materials for siRNA therapeutics. *Nat Mater*. 2013;12(11):967-977.
22. Zordev Khvalevsky E, Gabai R, Rachmut IH, et al. Mutant KRAS is a druggable target for pancreatic cancer. *Proc Natl Acad Sci U S A*. 2013;110(51):20723-8.
23. Rozema DB, Lewis DL, Wakefield DH, et al. Dynamic PolyConjugates for targeted in vivo delivery of siRNA to hepatocytes. *Proc Natl Acad Sci U S A*. 2007;104(32):12982-7.
24. McNamara JO 2nd, Andrechek ER, Wang Y, et al. Cell type-specific delivery of siRNAs with aptamer-siRNA chimeras. *Nat Biotechnol*. 2006;24(8):1005-1015.
25. Meade BR, Dowdy SF. Exogenous siRNA delivery using peptide transduction domains/cell penetrating peptides. *Adv Drug Delivery Rev*. 2007;59(2-3):134-140.
26. Cuellar TL, Barnes D, Nelson C, et al. Systematic evaluation of antibody-mediated siRNA delivery using an industrial platform of THIOMAB-siRNA conjugates. *Nucleic Acids Res*. 2015;43(2):1189-1203.
27. Debacker AJ, Voutilainen J, Catley M, Blakey D, Habib N. Delivery of oligonucleotides to the liver with GalNAc: from research to registered therapeutic drug. *Mol Ther*. 2020;28(8):1759-1771.
28. Peer D, Zhu P, Carman CV, Lieberman J, Shimaoka M. Selective gene silencing in activated leukocytes by targeting siRNAs to the integrin lymphocyte function-associated antigen-1. *Proc Natl Acad Sci U S A*. 2007;104(10):4095-4100.
29. Nagasaka M, Li Y, Sukari A, Ou SI, Al-Hallak MN, Azmi AS. KRAS G12c game of thrones, which direct KRAS inhibitor will claim the iron throne? *Cancer Treat Rev*. 2020;84:101974.
30. Sreedurgalakshmi K, Srikanth R, Rajkumari R. CRISPR-Cas deployment in non-small cell lung cancer for target screening, validations, and discoveries. *Cancer Gene Ther*. 2020;28(6):566-580.
31. Deng X, Wang Y, Zhang F, et al. Acidic pH-induced charge-reversal nanoparticles for accelerated endosomal escape and enhanced microRNA modulation in cancer cells. *Chem Commun (Camb)*. 2016;52(15):3243-3246.
32. Rayamajhi S, Marchitto J, Nguyen TDT, Marasini R, Celia C, Aryal S. pH-responsive cationic liposome for endosomal escape mediated drug delivery. *Colloids Surf B Biointerfaces*. 2020;188:110804.
33. Kushibiki T, Tomoshige R, Iwanaga K, Kakemi M, Tabata Y. In vitro transfection of plasmid DNA by cationized gelatin prepared from different amine compounds. *J Biomater Sci Polym Ed*. 2006;17(6):645-658.
34. Hosseinkhani H, Aoyama T, Ogawa O, Tabata Y. Ultrasound enhancement of in vitro transfection of plasmid DNA by a cationized gelatin. *J Drug Target*. 2002;10(3):193-204.
35. Santoro M, Tatara AM, Mikos AG. Gelatin carriers for drug and cell delivery in tissue engineering. *J Control Release*. 2014;190:210-218.
36. Carvalho JA, Abreu AS, Ferreira VTP, et al. Preparation of gelatin nanoparticles by two step desolvation method for application in photodynamic therapy. *J Biomater Sci Polym Ed*. 2018;29(17):1287-1301.
37. Kim MT, Chen Y, Marhoul J, Jacobson F. Statistical modeling of the drug load distribution on trastuzumab emtansine (Kadcyla), a lysine-linked antibody drug conjugate. *Bioconjug Chem*. 2014;25(7):1223-1232.
38. Baumer N, Appel N, Terheyden L, et al. Antibody-coupled siRNA as an efficient method for in vivo mRNA knockdown. *Nat Protoc*. 2016;11(1):22-36.

39. Sunaga N, Shames DS, Girard L, et al. Knockdown of oncogenic KRAS in non-small cell lung cancers suppresses tumor growth and sensitizes tumor cells to targeted therapy. *Mol Cancer Ther.* 2011;10(2):336-346.
40. Srikar R, Suresh D, Zambre A, et al. Targeted nanoconjugate co-delivering siRNA and tyrosine kinase inhibitor to KRAS mutant NSCLC dissociates GAB1-SHP2 post oncogene knockdown. *Sci Rep.* 2016;6:30245.
41. Hoeben A, Martin D, Clement PM, Cools J, Gutkind JS. Role of GRB2-associated binder 1 in epidermal growth factor receptor-induced signaling in head and neck squamous cell carcinoma. *Int J Cancer.* 2013;132(5):1042-1050.
42. Yanagi T, Shi R, Aza-Blanc P, Reed JC, Matsuzawa S. PCTAIRE1-knockdown sensitizes cancer cells to TNF family cytokines. *PLoS One.* 2015;10(3):e0119404.
43. Al Nakouzi N, Wang CK, Beraldi E, et al. Clusterin knockdown sensitizes prostate cancer cells to taxane by modulating mitosis. *EMBO Mol Med.* 2016;8(7):761-778.
44. Chen S, Evans HG, Evans DR. FLASH Knockdown sensitizes cells to Fas-mediated apoptosis via down-regulation of the anti-apoptotic proteins, MCL-1 and Cflip short. *PLoS One.* 2012;7(3):e32971.
45. Tushir-Singh J. Antibody-siRNA conjugates: drugging the undruggable for anti-leukemic therapy. *Expert Opin Biol Ther.* 2017;17(3):325-338.
46. Nanna AR, Kel'in AV, Theile C, et al. Generation and validation of structurally defined antibody-siRNA conjugates. *Nucleic Acids Res.* 2020;48(10):5281-5293.
47. Xia CF, Boado RJ, Pardridge WM. Antibody-mediated targeting of siRNA via the human insulin receptor using avidin-biotin technology. *Mol Pharm.* 2009;6(3):747-751.
48. Sugo T, Terada M, Oikawa T, et al. Development of antibody-siRNA conjugate targeted to cardiac and skeletal muscles. *J Control Release.* 2016;237:1-13.
49. Chernikov IV, Vlassov VV, Chernolovskaya EL. Current development of siRNA bioconjugates: from research to the clinic. *Front Pharmacol.* 2019;10:444.
50. Sinha SK, Asotra K, Uzui H, Nagwani S, Mishra V, Rajavashisth TB. Nuclear localization of catalytically active MMP-2 in endothelial cells and neurons. *Am J Transl Res.* 2014;6(2):155-162.
51. Tai W, Gao X. Functional peptides for siRNA delivery. *Adv Drug Delivery Rev.* 2017;110-111:157-168.
52. Metwally AA, Pourzand C, Blagbrough IS. Efficient gene silencing by self-assembled complexes of siRNA and symmetrical fatty acid amides of spermine. *Pharmaceutics.* 2011;3(2):125-140.
53. Healey GD, Frostell A, Fagge T, Gonzalez D, Conlan RS. A RAGE-targeted antibody-drug conjugate: surface plasmon resonance as a platform for accelerating effective ADC design and development. *Antibodies (Basel).* 2019;8(1):7.
54. Zwaagstra JC, Sulea T, Baardsnes J, et al. Binding and functional profiling of antibody mutants guides selection of optimal candidates as antibody drug conjugates. *PLoS One.* 2019;14(12):e0226593.
55. Kim GP, Grothey A. Targeting colorectal cancer with human anti-EGFR monoclonal antibodies: focus on panitumumab. *Biologics.* 2008;2(2):223-228.
56. Sickmier EA, Kurzeja RJ, Michelsen K, Vazir M, Yang E, Tasker AS. The panitumumab EGFR complex reveals a binding mechanism that overcomes cetuximab induced resistance. *PLoS One.* 2016;11(9):e0163366.
57. Yang S, Liu G. Targeting the Ras/Raf/MEK/ERK pathway in hepatocellular carcinoma. *Oncol Lett.* 2017;13(3):1041-1047.
58. Aksamitiene E, Kiyatkin A, Kholodenko BN. Cross-talk between mitogenic Ras/MAPK and survival PI3K/Akt pathways: a fine balance. *Biochem Soc Trans.* 2012;40(1):139-146.
59. Sun YJ, Zhuo ZL, Xian HP, Chen KZ, Yang F, Zhao XT. Shp2 regulates migratory behavior and response to EGFR-TKIs through ERK1/2 pathway activation in non-small cell lung cancer cells. *Oncotarget.* 2017;8(53):91123-91133.
60. Furcht CM, Munoz Rojas AR, Nihalani D, Lazzara MJ. Diminished functional role and altered localization of SHP2 in non-small cell lung cancer cells with EGFR-activating mutations. *Oncogene.* 2013;32(18):2346-2355. 55 e1-10.
61. Lazzara MJ, Lane K, Chan R, et al. Impaired SHP2-mediated extracellular signal-regulated kinase activation contributes to gefitinib sensitivity of lung cancer cells with epidermal growth factor receptor-activating mutations. *Cancer Res.* 2010;70(9):3843-3850.